Scale Levels of Crack Closure Effects and Simulation of Fatigue Cracking of Al-based Sheet Materials Subjected to Biaxial Cyclic Loads

A.A.Shanyavskiy

State Centre for Civil Aviation Flights Safety, 141426, Moscow Region, Chimkinskiy State, Airport Sheremetievo-1, P.O. Box 54, Moscow, Russia, shananta@stream.ru

ABSTRACT. Fatigue crack growth experiments were carried out on cruciform specimens in the range of thickness 1.2 to 10 mm of Al-based alloys, loaded under regular and irregular uniaxial and biaxial loads, including sequences of various overloads. Different cases for crack closure effects were considered because of shear lips development, crack growth direction re-orientation after multiparameters change of cyclic loads, considering plastic blunting effect at a crack tip during an overload, and interaction effects by analyzing the crack retardation length and associated parameters together with their relationships. Crack closure effect because of rotation instability of material meso-volumes under biaxial compression-tension has been suggested for semi-elliptical cracks. Under biaxial cyclic loads in the range of load ratios $-1.4<\lambda<+1.5$, in the range of R-ratios 0.05 to 0.8, for frequency variations ϖ, fatigue striation formation took place beyond a crack growth rate near to $4\text{x}10^{-8}$ m/cycle. The striation spacing and the crack growth rate increase as the ϕ-angle of the out-of-phase biaxial loads increase in the range of ϕ-angles from 0^0 to 180^0. Cyclic loading parameters must be taken into account in order to describe the crack growth period when using a unified method that involves an equivalent stress intensity factor $K_e = K_I F(\lambda, R, \phi, \varpi)$. The values of $F(\lambda, R, \phi, \varpi)$ were determined. The calculated crack growth period (predicted using the $F(\lambda, R, \phi, \varpi)$) in regular and irregular cases of cyclic loads, including material cracking after overloads, is correlated with the experimental data and the error is of the order of 15%.

INTRODUCTION

Many aircraft components in flight have experienced a biaxial stress-state resulting from external loads Shanyavskiy [1,2]. The stress-state developed in a local area results from external interaction of axial, bending, shear, and torsion stresses and can be biaxial along with local peak stress cycle variations. They are in-phase if both stresses have the same sense relative to their mean, and out-of-phase if they have an opposite sense relative to their mean values. They are out-of-phase for other combinations in time between the maximum values of principal stress σ_1 and σ_2. A special investigation of the

stressed states of components during flights has shown Shanyavskiy [1] all the various kinds of out-of-phase cycling, Fig.1, and in some stages of these cycles the angle ϕ between the vectors of the σ_1 and σ_2 stresses can vary up to ϕ=90^0.

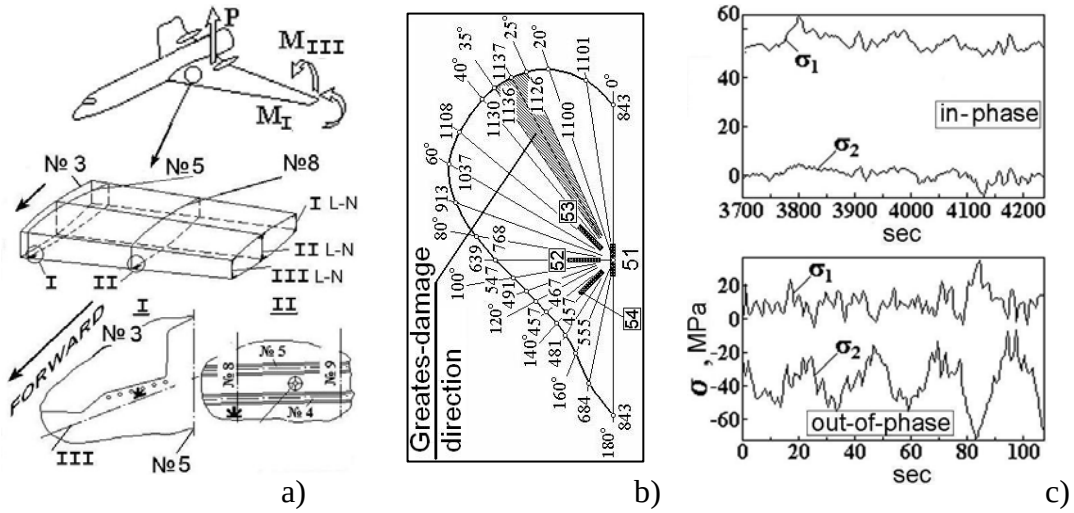

a) b) c)

Figure1. Schematic of a YaK-42 aircraft with strain gage positions (a) in the center-plane, (b) and (c) diagrams of strain-gage signals, given in loading-cycle units, received during typical flights of a YaK-42 plane from the monitoring zones arranged in various directions and numbered from No3 through No9. The shaded zones in (b) coincide with the orientation of the first principal stress and represent the sites of greatest accumulated damage.

In-phase biaxial loads have been used to analyze fatigue crack growth from a central hole of cruciform specimens of Al-based sheet materials Shanyavskiy [3-6]. The fatigue crack growth in this case can be considered on the basis of the well-known criterion Miller [7] for the determination of stress intensity factors from knowledge of plastic zone sizes when various external loads are applied to a component (because the plastic zone size decreases, the growth rate decreases as the stress ratio $\lambda = \sigma_2 / \sigma_1$ increases).

Investigations carried out for regular and irregular cyclic loads of Al-based alloys [3-6, 8-10], had shown similar crack growth behaviour for uniaxial and biaxial loads at various R-ratios. At the same time various mechanisms were seen for different λ-ratios, which mainly confirmed the biaxial overload influence on crack growth Shanyavskiy [9]. The influence of regular biaxial cyclic loads on the fatigue crack growth rate can be expressed in the following form Shanyavskiy [2]:

$$da/dN = \begin{Bmatrix} C_1 \\ C_s \\ C_2 \end{Bmatrix} K_e^m \begin{Bmatrix} m=4 \\ m=2 \\ m=4 \end{Bmatrix} for \begin{Bmatrix} da/dN > 4.75x10^{-8} m/cycle \\ 4.75x10^{-8} m/cyle < da/dN < 2.14x10^{-7} m/cyle \\ 2.14x10^{-7} m/cycle \end{Bmatrix} \begin{matrix} (1) \\ (2) \\ (3) \end{matrix}$$

In the Eqs. (1)-(3) the proportionality factors for through-thickness cracks are $C_s = [1-\nu^2]/[12E\sigma_{0.2}]$, $C_1 = C_s / K_{e1}^2$, and $C_2 = C_s / K_{es}^2$. Values of K_{e1} and K_{es} correlate to values of growth rate of 4.75x10^{-8}m/cyle and 2.14x10^{-7}m/cycle respectively.

The stress intensity effective or equivalent factor, K_e, has been introduced to describe fatigue crack growth in components on the basis of the Miller-criterion [7] plus a synergistic approach Shanyavskiy [1,2]:

$$K_e = K_I [1 + \sum_{i=1}^{k} f(X_i)]^{1/2} = K_I F(X_1, X_2 ... X_i) \qquad (4)$$

There are X_i parameters of external cyclic loads in Eq. (4) that increase or decrease crack growth compared with the standard situation of an uniaxial tension with R=0 when the stress intensity factor K_I has been determined for σ_1 value. The stress intensity equivalent factor, K_e, is that which gives the same value of the fatigue crack growth rate for a wide range of variation of external cyclic loads. In the case of biaxial cyclic loads with various R-ratios and ϕ- angles it should give the same crack growth rate for the cyclic loading parameters λ_1, R_1, ϕ_1 and λ_2, R_2, ϕ_2. Hence, the correction function is constant and equal to one under equivalent conditions. This indicates the possibility of describing the crack growth rate at different λ, R, ϕ values with one kinetic curve according to which the growth rate depends on the value of an equivalent stress intensity factor $K_e = F(\lambda, R, \phi)$, where $F(\lambda, R, \phi)$ is a dimensionless correction function of the stress intensity factor for various biaxial stress-state.

The function correction $F(\lambda, R, \phi)$ in fatigue tests must be determined under uniformly biaxial cyclic loads. That is why, the specimen sizes optimization was performed to realize the central part with a permanent R-ratio within several tens millimeters diameter based on the finite element analysis Shanyavskiy [3-6].

The semi-elliptic fatigue crack growth is not the same as that found for the through crack, as shown by recent results [11, 12]. It penetrates the specimen section in the depth direction and simultaneously grows along the specimen surface. The specimen thickness for the crack size in the depth direction has to be enough for the crack size to be several tens of millimeters on the specimen surface. This situation can be exceeded for the thick specimen with the thickness greater than 10mm. The gripped specimen ends have to be thicker than the central part of the specimen in order to realize a sufficient maximum principal stress level during the regular cyclic loads.

Fatigue crack growth after an overload depends on the overload level, principal stress level σ_1, stress intensity factor, λ-ratio, R- ratio, specimen thickness and other

parameters Shanyavskiy [1]. However, all well-known models of fatigue crack growth, which have been developed for the case of uniaxial overloads, can be expressed in the following form:

$$(da/dN) = C_t \ (da/dN)_0 \tag{5}$$

In Eq.(5) the factor C_t includes all parameters influencing the growth rate after an overload as a result of cyclic loads interaction effects, and $(da/dN)_0$ correlates to the crack growth rate without an overload. The stress intensity factor K_e takes into account many factors influencing growth rate at a regular cyclic load, i.e. frequency, temperature, environment and others.

But in the case of very frequently introduced overloads the dominant role for interaction effects of cyclic loads is on the process of plastic deformation of material at the crack tip, which influences the crack increment. The model simulated fatigue crack growth under irregular biaxial cyclic loads has to use knowledge about this process.
The paper presented analyses of scale levels for crack closure effects on cruciform specimens made from Al-based alloys, which were used for cyclic loading tests under biaxial loads with various λ - ratios, *R*-ratios, ϕ-angles, and frequencies ϖ. Investigations carried out for regular and irregular biaxial cyclic loads of AK4-1T1, D16T and AK6 Al-alloys, having thicknesses 1.2, 2, 4.9, and 10 mm, Shanyavskiy [3], [4], [6]. A model of crack growth under regular cyclic loads and under sequence of of cycles with overloads in the case of biaxial loads is discussed based on different crack closure effects which take place on different scale levels.

CRACK GROWTH SIMULATION UNDER REGULAR CYCLIC LOADS

Plane-stress conditions for crack closure effect

In this case, investigations have been developed for the thin sheet material of AK4-1T1 Shanyavskiy [3]. Specimen thicknesses were 1.2 and 2mm. A central hole of 2mm in diameter was used as a stress raiser. A flat slit of 1mm in depth was prepared in both directions from the central hole at angles of 90^0 and 45^0 to the direction of the principal stress σ_1 for λ =+1.0. In other cases the flat slit was perpendicular to the stress σ_1. The cyclic loading parameters for the maximum value of σ_1, and λ-ratio were 42…113 MPa and -1.0; -0.5; 0; +0.5; +1.0 respectively at *R*=0.5.

The fatigue surface in the interior does not deviate too far from the horizontal plane for the range of $-1.0 < \lambda < 0$. The crack has a change in its orientation to the horizontal axis of 30^0 in the case of λ =+0.5. The crack orientation was always at 45^0 to the principal stress σ_1 in the interior where material cracking takes place in Mode I with fatigue striation formation. The difference in crack path between the specimen surface and the interior exists because of shear lip formation at the specimen surface. This phenomenon

influenced crack closure and has to be considered for equivalent stress intensity factor K_e determination.

The functional correction $F(\lambda, R)$ was calculated for thin sheets in the case of spontaneous crack growth direction re-orientation under various λ-ratio under plane-stress conditions. Fatigue crack propagation because of fatigue striation formation can be uniformly simulated for different levels of stress σ_1 and various λ-ratios, influencing various situations with crack closure effect, based on knowledge of K_e values and the calculated functional correction $F(\lambda, R)$, Fig.2. For example, kinetic curves in terms of K_e are similar when the crack orientation is parallel or at 30^0 to the horizontal axis at λ=0 and λ=0.5 respectively.

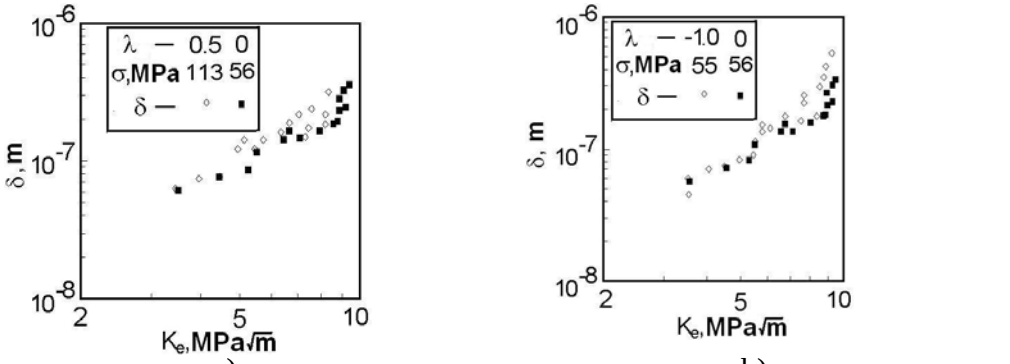

a) b)

Figure 2. Unified fatigue striation spacing, δ, dependencies on the equivalent stress intensity factor, K_e, for different cyclic loading parameters.

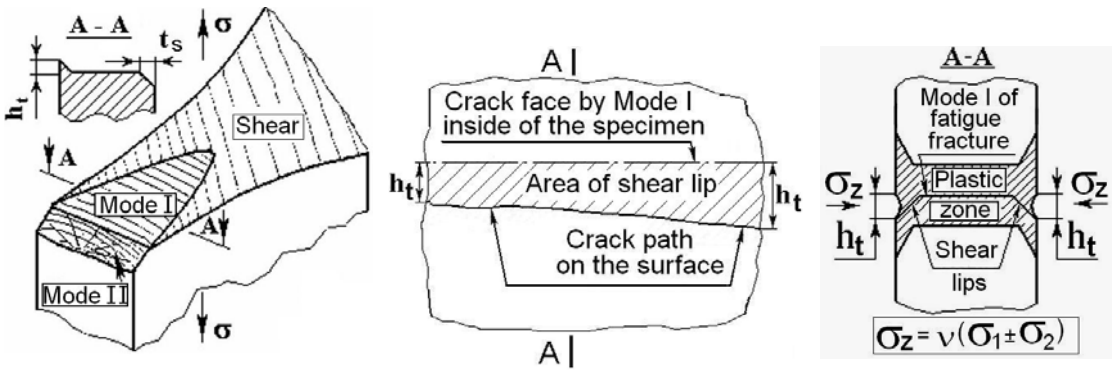

a) b) c)

Figure 3. Parameters of the fracture surface (a) of a through fatigue crack in the transition from the tensile mode to the shear mode, and (b) – (c) schematic of shear lip and plastic zone areas in the case of biaxial cyclic loads.

Plane-strain conditions for crack closure effect

The transition from tensile-to-shear mode crack growth under uniaxial cyclic tensile stress, leading to the development of shear lips along the edges of the fracture surface in Al-alloy sheet and plate materials is a well-known phenomenon Shanyavskiy [1]. The shear lips can be characterized by three dimensions, Fig.3, (a) the width t_s, (b) the height h_t, (c) and diagonal s.

These dimensions are evidence of local plane stress conditions along the front of the crack while the tensile mode area of width in the middle area of the specimen corresponds to a plane strain condition. A similar situation exists for fatigue crack fronts under biaxial tension or tension-compression cyclic loads Shanyavskiy [2].

For crack growth under uniaxial cyclic tensile stress at R values from 0 to 0.6 in air, the shear lip width t_s was approximately proportional to ΔK_{eff}^2, Schijve [13], where ΔK_{eff}, defined in [14], is based on crack opening and can be written as $\Delta K_{eff} = K_I F(R)$, where $F(R)$ is a correction function of the stress intensity factor for various R values. During fatigue crack growth, from a viewpoint of synergetics Shanyavskiy [1,2], one can describe any multi-parametric effect on fatigue crack growth using unified method of K_e, i.e. an equivalent stress intensity factor which determines the behavior of fatigue cracks.

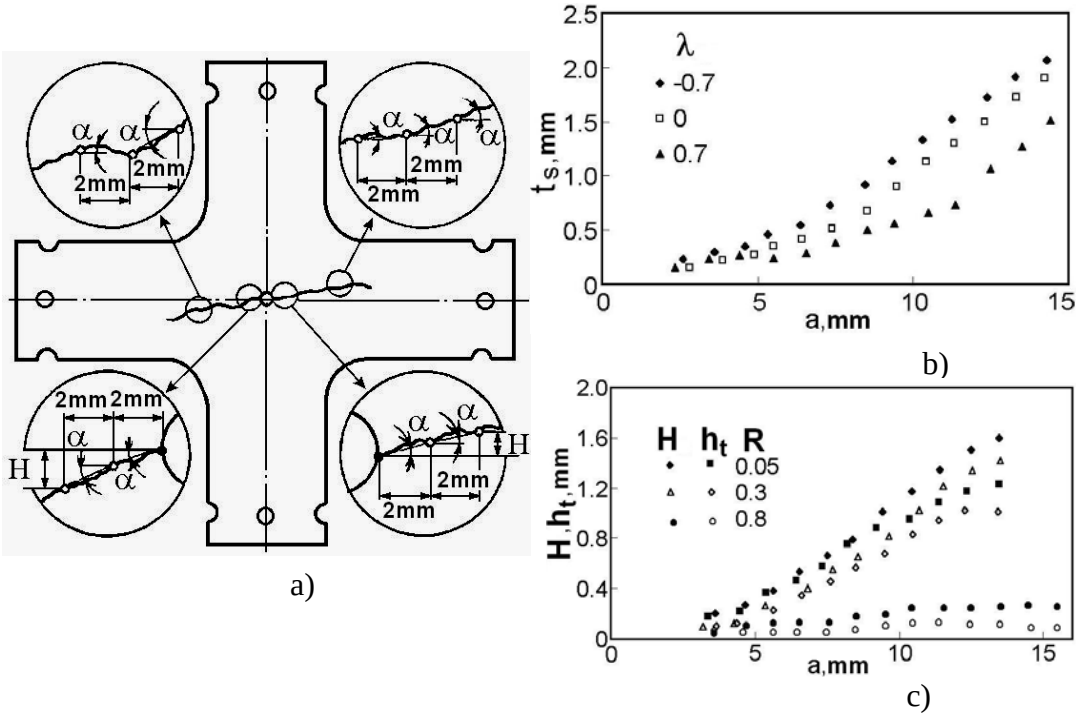

Figure 4. Shear lip (a) parameters α (angle) and H (height) which were measured on the cruciform specimen, and (b), (c) dependencies of shear lip parameters H and h_t on crack length a for the aluminium alloy D16T at various λ and R ratios.

In the biaxial case of cyclic loading measurements of shear lip dimensions were made on specimens of Al-alloy D16T (equivalent to 2024 T3), having a sheet thickness 4.9 mm, and tested at λ-values from -1.4 to +1.5 and at R-values from 0.05 to 0.8.

The shear lip H-value, Fig.4, was obtained and the angle α measured on the specimen surface.

Then H-values and h_t-values were compared. The difference between these values was not significant. The direction of crack growth in the interior was horizontal, and in the x-axis direction, at all the λ and R values. This direction of crack growth is approximately normal to the direction of the tensile stress σ_1.

It was shown that the fatigue fracture surface orientation depends not only on λ and R values at the inside but also on the specimen geometry. In aluminium sheet materials with the central notch plane normal to the tensile stress σ_1 direction there was no difference in the interior crack growth direction in respect to the λ value if the sheet thickness t is greater than 4.9 mm. Between $2<t<4.9$ mm a transition to a dependence on the λ value is realized. The plane stress condition determined the dependence effect of the fatigue crack growth orientation on the λ value. It seems to be that this situation applies to any material and not only Al-alloys.

The formation of shear lips exhibits a systematic behaviour. That is why a unified kinetic diagram was constructed and has the description

$$t_s = \begin{Bmatrix} 8.4x10^{-7} \\ 3.08x10^{-9} \end{Bmatrix} K_e^m \begin{Bmatrix} m=2 \\ m=4 \end{Bmatrix} \begin{Bmatrix} t_s < 2.5x10^{-4} m \\ t_s > 2.5x10^{-4} m \end{Bmatrix} \tag{6}$$

$F(\lambda,R)$ values were calculated when examining the effect of any of the loading cycle parameters. The relations found were:

$$F(R) = [1 - 1.39R - 1.11R^2 + 4.14R^3 - 3.16R^4]^{1/4} \quad \text{, when } \lambda = 0 \tag{7}$$

$$F(\lambda) = [1 - 0.719\lambda - 0.314\lambda^2 + 0.162\lambda^3 + 0.25^4]^{1/4} \text{, when } R=0 \tag{8}$$

The tensile fracture mode in the interior of specimens does not change at various λ and R values (fatigue striations are formed on the fracture surface) and crack opening in the σ_1 direction involve combined modes I and III opening at the shear lip. Therefore, the crack closure effect being the result of shear lips development is determined by the unified process of deformation near the crack tip at the specimen surface under any multiaxial cyclic loads, when fatigue striations in the interior of the specimen are formed.
Loading cycle parameters do not influence the transition fracture processes from the sheet interior (plane strain) to the material surface (plane stress). That is why the shear lip t_s values are an integral characteristic of material reaction to multiaxial cyclic loads.

Meso-scale level of crack closure effect

The influence of loading condition on the stress state of the material at the through crack tip manifests itself in terms of energy spent on crack propagation as λ and R ratios change. The decisive role in fatigue crack development concerns mode I crack opening. The through-crack propagation is characterized by a decrease of the plastic zone size at the crack tip if the λ-ratio is increased Miller [7]. Therefore a decrease in growth rate and striation spacing suggests that the plastic zone size decreases. As a result the crack growth period increases as the λ-ratio increases in the range $-1.0<\lambda<+1.0$. It was confirmed for the sheets of aluminium alloys in the range of thickness $1.2<t<4.9$ mm Shanyavskiy [3-5].

Semi-elliptic cracks are repeatedly found on in-service failure surfaces of cyclically loaded structural components. In fact, such cracks typically start as semi-elliptical ones. In a plate or cruciform specimen, as shown in [1, 6, 11, 12], a σ_2 stress component is conventionally applied normal to the crack-opening stress, i.e., along the surface in which the semi-elliptic crack must nucleate and grow, Fig.5. Two alternatives of the σ_2 direction are to be considered with respect to a semi-elliptic surface crack, viz. normal and parallel to the surface at which the crack was nucleated.

When σ_2 is applied in the specimen-thickness direction (normal to the specimen surface), the condition are obeyed particularly for the growth of a through crack when the λ magnitude correlates with crack-growth rates both in the through and in the surface direction. Yet with the σ_2 applied parallel to the specimen surface, it is the plastic-zone size that correlates with the crack-growth rate of both semi-elliptic and through cracks. These are basic considerations of fatigue-fracture mechanics.

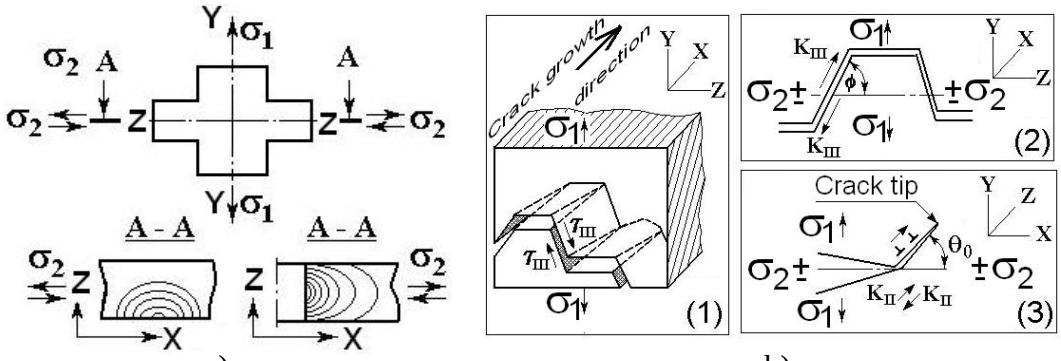

c) b)

Figure 5. Schematics (a) of a plate under external biaxial loading with semi-elliptical and through cracks, and (b) of "mesotunnels" (1) formation in the crack growth direction that can have different influences (2), (3) of the σ_2 stress on the crack propagation.

Fatigue tests of cruciform specimens in 10 mm of thickness of AK6 aluminium alloy have shown that in the case schematized in Fig.5a and (2), a negative-to-positive transition of λ ensured, for the same σ_1 level, an increased crack-growth rate.

To understand why the growth rates of semi-elliptical and through fatigue cracks show opposite dependencies with positive λ, one should note the different orientations of the mesotunnels (see Fig.5) with respect to the σ_2 axis. In our tests, the mesotunnels axes were mostly directed normal to the σ_2 axis (case (2) in Fig.5b). The mesotunnels were the first step in the crack initiation event and served as a border region between neighbouring volumes of the fractured metal. Two fracture modes were possible, Fig.6. Generally it was fracture by the τ_{III}-mode.

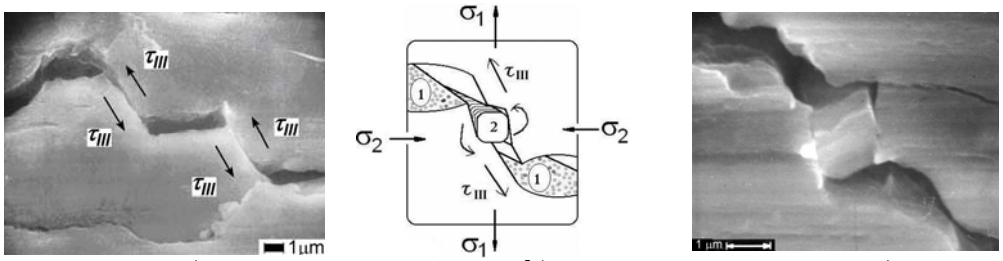

a) b) c)

Figure 6. Fracture development (a), (c) at the notch tip under biaxial loading, and (b) schematic process presented in (c). Prior fracture zones (tunnels "1"), have formed by mode I crack opening. The intertunnel "bridges" break by a τ_{III}-mode (shear) or by τ_{III}-mode rotation.

Yet the rotation-instability fracture mode was also possible, which would ensure the formation of cylindrical particles in-between the newly formed free crack surface of the metal. Due to mode III-shear, the cylindrical particles could then be reshaped to spherical ones by rolling or twisting between crack surfaces under cyclic loads.

Obviously, the intertunnel metal will fracture more easily with increasing σ_2, which can finally ensure the total suppression of the mesotunnel fracture mode too. Below this σ_2 level, a tunnel will be shallow. In other words, an increase of λ facilitates metal fracture, and the cracks must grow faster thanks solely to an increase in σ_2. At negative λ (negative σ_2), the intertunnel-metal fracture is hampered and, hence, plastic rotation instability of the metal volumes is preferred.

In the through-crack case, the tunnels mostly extend parallel to the σ_2 axis from the very beginning of the semi-elliptic-crack growth, whatever the λ sign. With a tensile σ_2 parallel to the crack-growth direction (see Fig.5b, (3)), the breakdown of the intertunnel crosspieces will be delayed owing to the Poisson effect (see Fig.3c) because the mesotunnels close under a positive λ.

However, the similarity of crack-growth behaviour at different λ magnitudes makes it possible to use a single kinetic curve, Eqs. (1) to (3), to account for crack-growth effects in AK6 alloy under biaxial loading. In the case discussed for semi-elliptical crack growth simulation, the correction function was expressed in the form:

$$F(\lambda) = (1 + 0.4\lambda + 0.28\lambda^2)^{1/2}, \text{ where } R=0.1 \quad (9)$$

Crack closure effect under out-of-phase loading

In-phase biaxial loads have been used to analyze fatigue through-crack growth from a central hole of a cruciform specimen Shanyavskiy [15]. Out-of-phase of biaxial loading has also been studied on cruciform specimens of D16T Al-alloy at the stress ratio R=0.3 over the λ-ratios: +0.3 (σ_1=125 MPa); -0.3 (σ_1=125 MPa); -0.5 (σ_1=115 MPa); +0.5 (σ_1=90 MPa). The crack-opening σ_1 stress, was first applied to the specimen at a test frequency of 5 Hz. Then the second stress, σ_2, was applied to the specimen, realizing the out-of-phase biaxial loading in the range of angles 0^0-300^0. The **Lissajou** figure controlled the out-of-phase angle, ϕ, between stresses.

The correction function $F_1(\lambda, R)$ values were determined for in-phase biaxial loading Shanyavskiy [5]. That is why only a function correction $F_2(\phi)$ has to be calculated for similar conditions of fatigue crack growth.

In the mid part of the specimen section, the crack plane does not deviate far from the horizontal plane at any λ-ratio and ϕ- angle. The striation spacing decreases for out-of-phase loading as this increases up to ϕ=180^0. It was only in out-of-phase loading when the striation spacing and growth rate had maximum values for a given crack length. Crack closure effect because of contact between crack edges was not found. The stress ratio R=0.3 explains this observation, crack edges were opened during loading and unloading portions of cyclic loads. The phase alteration only influenced the energy dispersal near the crack tip. The crack opening process does not change as the crack develops.

The out-of-phase angle is one of the parameters in biaxial loading that can be considered as having an energetic influence on the process of plastic deformation developed at a crack tip in a loading cycle. The plastic zone size increases as the ϕ-angle increases in the range $0^0 < \phi < 180^0$. Then this zone decreases as the ϕ-angle further increases.

Therefore, the crack which develops for in-phase and out-of-phase biaxial loads is similar in cruciform specimens having a thickness of approx. 5 mm and so a unified description of fatigue crack growth was considered to simulate material cracking based on Eqs. (1) to (3) and using the dimensionless correction function $F_2(\phi)$ that has been calculated.

CRACK GROWTH SIMULATION UNDER IRREGULAR CYCLIC LOADS

Macro level of crack closure effect because of plastic zone re-orientation

Irregular cases of cyclic load sequences can be realized because of mainly principal stress level σ_1 or λ-ratio variations. More complicated cases are related to simultaneously varying all parameters in combinations of $\sigma_1, \lambda, R, \varpi$, where ϖ-frequency. The

cases discussed were examined for several sequences of cyclic loads Shanyavskiy [5]: (1) Blocks of cyclic loads with overload factors 1.5 and 1.8 for λ-ratios -0.7, +0.2, and +0.7 at σ_1 = 140 MPa; (2) Blocks of loads modulated by a sinusoidal law of amplitude variation with a period of 12 cycles at a frequency of 8Hz for λ-ratios +0.2, and +0.7; (3) Blocks of different λ-ratios had two sequences - -0.2; -0.4; -0.7; -1.0; -1.4, and +0.2; +0.4; +0.7; +1.0, and +1.4; 4. A single transition from one combination of $(\sigma_1, \lambda, R)_i$ to another with simultaneous changes to their values in the ranges -1.4< λ <+1.4, 0.2<R<0.7, and 120< σ_1 <240MPa. Frequency ϖ has changed from 0.5 to 5 Hz and, conversely, from 5 to 0.5 Hz. Tests were developed on the cruciform specimens, having a sheet thickness of 5mm, from the D16T Al-alloy.

It was found that different sequences of cyclic loads lead to different values of the functional correction *F(λ,R)* compared to that for the regular case of various combinations of λ,*R*. For example, the correction function *F(λ,R=0)* for the 1-sequence of cyclic loads in a block increases by a factor of about 1.1, decreasing or increasing respectively as stress levels in the block decrease or increase.

In all cases studied there was no significant difference between values for situations when fatigue striations had formed after transition from one combination of σ_1, λ, R parameters to another.

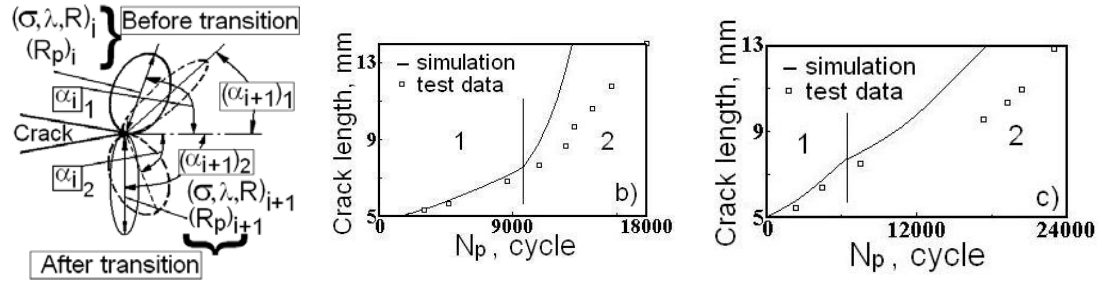

a)

Figure 7. Schematic (a) of the plastic zone re-orientation after transition for one combination of $(\sigma_1, \lambda, R)_i$ parameters to another $(\sigma_1, \lambda, R)_{i+1}$, and (b), (c) dependencies of crack length on number of cycles found in tests and simulated using functional correction values calculated for regular cyclic loads: (b) $(\sigma_1, \lambda, R)_1$ – (120 MPa, -0.4, 0.4); $(\sigma_1, \lambda, R)_2$ – (240 MPa, +0.4, 0.2); (c) $(\sigma_1, \lambda, R)_1$ – (200 MPa, 0.7, 0.3); $(\sigma_1, \lambda, R)_2$ – (150 MPa, 0.4, 0.4).

That is why the unified kinetic diagram, Eqs (1) to (3), was used to simulate material fatigue cracking with the same functional correction values as those obtained for regular cyclic loads Shanyavskiy [5]. The results obtained only showed good agreement between simulated and experimental numbers of cycles for cases of drastically increased λ-ratios (from +0.4 or -0.4 to +1.4) especially when simultaneously increasing the principal stress σ_1 from 150MPa to 240MPa. For example, *F(λ,R)* by a factor of three or

two times under σ_1=200MPa for transitions from combination of λ,R: -0.7, 0.4 to +0.4, 0.3, or from λ,R: -0.4,0.4 to +0.4, 0.2 respectively. In the cases of irregular λ-ratio discussed there is a crack closure effect because of the difference in plastic zone orientation ahead of a crack tip before and after changes of parameters in combinations of σ_1, λ, R, Fig.7.

Interaction effects of cyclic loads have to be considered because of variations in plastic zone size and its orientation. Fracture surface analyses have shown small deviation of crack growth direction after transition from one combination of σ_1, λ, R parameters to another. However, the main orientation was the same before and after the transition discussed. Tilting of crack path after the transitions discussed reflected the interaction effect of cyclic loading parameters that delayed cracking and decreased crack growth rates. Re-orientation of the plastic zone ahead of a crack tip played a positive role in the material cracking process by decreasing crack closure in the main direction of material cracking. That is why it can be recommended to simulate cracking of sheet materials under different combinations of σ_1, λ, R parameters when after transition to new combination $(\sigma_1, \lambda, R)_{i+1}$ there is no change in the mechanism of material cracking.

Scale levels for crack closure effects because of overloads

The influence of overloads on fatigue crack growth in uniaxial tension of sheet materials is a well-known phenomenon [16-18]. Many relations were introduced for the fatigue crack simulation in the case of a number of cycles between overloads, which are sufficient for the crack to traverse the plastic zone produced by an overload. During an overload there is plastic blunting at a crack tip in the mid section of specimens which develops a stretch zone at the meso scale level, Fig.8.

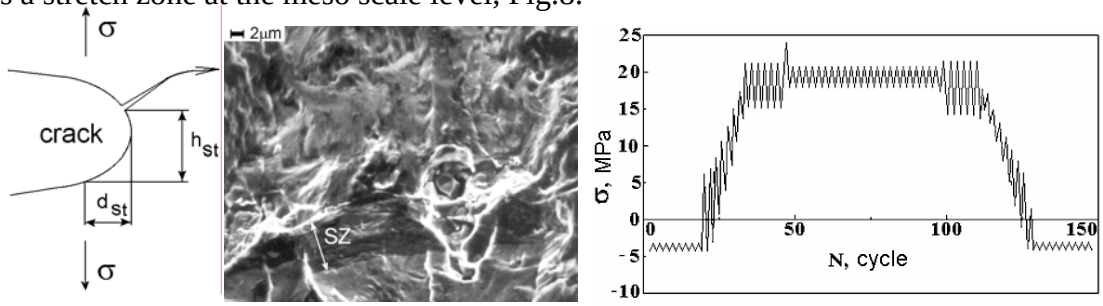

a) b) c)

Figure 8. Stretch zone (SZ) parameters (a) d_{st} and h_{st}, (b) overview on the SZ produced in a cruciform specimen of D16T Al-alloy subjected to an overload factor 2.1, λ=-0.2, R=0.3, and (c) typical sequence of cyclic loads in one block representing one flight for a schematic stress-state in one local area of a wing of the Yak-42 aircraft.

At the same time, on the macro scale level, after an overload, there is a sequence of events, at the specimen surface, in the plastic zone ahead of a crack tip, Fig.9. First, the

crack accelerates over the distance $(a_D)_{1-2}$, then the crack stops during N_D cycles, and new crack propagation inside the plastic zone produced during an overload influences the residual stresses created during an overload. The shear stress, τ_{III}, dominates the fracture process near the specimen surface immediately after an overload. It seems to be this "delayed retardation" effect which explains the tearing and seizure processes, that take place on the shear lip surface.

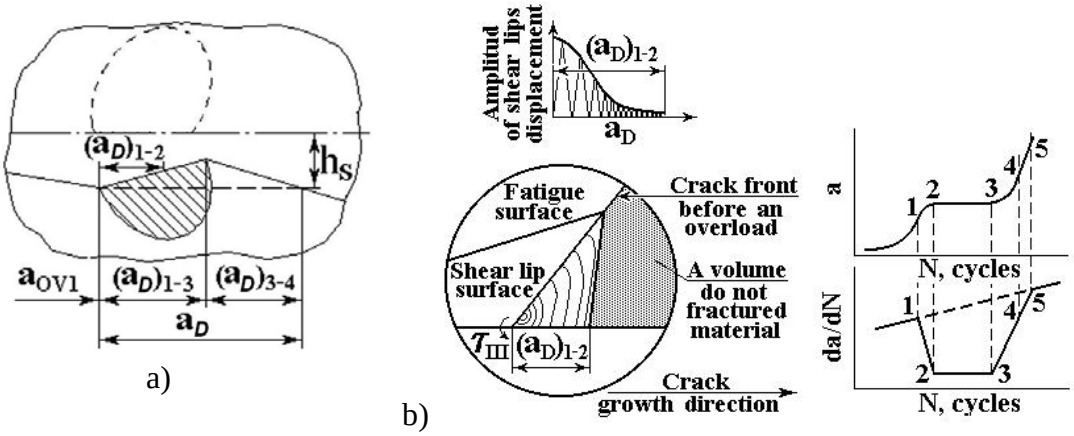

Figure 9. Schematic pictures of the plastic zone formation and different processes of crack development on the specimen surface (a) after an overload and (b) pictures of the developing crack topography near the specimen surface immediately after an overload.

A crack growth simulation of the case of a sequence of overloads was performed for cruciform specimens of approx. 5.0 mm in thickness. In the mid part of the test specimen with this thickness, the crack plane does not deviate too far from the horizontal plane at any λ-ratio. That is why the crack growth simulation is done without taking into consideration the deviation of the fracture plane from the horizontal plane for various λ-ratio. Therefore, the first step in numerical analysis for fatigue crack growth modelling was performed taking into consideration the functional correction $F(\lambda, R)$ for the case of through crack growth Shanyavskiy [3]. It was then used to calculate the equivalent stress intensity factor by Eqs. (1) to (4).

The plastic zone size, a_D, within which the load interaction effect after an overload can be seen, can be calculated on the basis of the maximum tensile deformation theory by the following relation Shanyavskiy [10]:

$$a_D = (a_D)_{\lambda=0}\,[0.25\lambda^2 - \lambda + 1][1.5 - R] \qquad (10)$$

The crack growth simulation must be derived from Eqs. (1) to (3) for various *R*- ratios in the range $0.1<R<0.5$ and $0<\lambda<0.7$ after an overload in the following form:

$$da/dN = \begin{Bmatrix} [(a_i - a_1)/a_{D12}][a_{D13} - a_{D12})/N_D - (da/dN)_1] + (da/dN)_1 \\ [a_{D13} - a_{D12}\}/0.9N_D = (da/dN)_{\min} \\ [(da/dN)_1 - (da/dN)_{\min}][a_i - (a_1 - a_{D13})]^2/[a_D - a_{D13}]^2 + \\ + (da/dN)_{\min} \end{Bmatrix} x$$

$$x[F_j(X_1; X_2 ... X_n)/F_1(X_1; X_2 ... X_n)]^2 ..... \begin{Bmatrix} a_1 \le a_i \le a_2 \\ a_2 \le a_i \le a_3 \\ a_3 \le a_i \le a_5 \end{Bmatrix} \begin{Bmatrix} (11) \\ (12) \\ (13) \end{Bmatrix}$$

In Eqs. (11) to (13) the $(da/dN)_1$ value correlates with the crack length, a_1, up to the moment of an overload, and $F_1(X_1; X_2 ... X_n)$, $F_j(X_1; X_2 ... X_n)$ correlate with the correction functions for the external cyclic loading parameters X_i up to the moment of an overload and for cycle-by-cycle after an overload respectively (see indications in Fig.9b).

The crack simulation developed by the relations (11) to (13) when the crack increment, Δ_f, during one-cycle estimates without calculation of the stretch zone. However, a realistic sequence of cyclic loads, which reproduced, for example, the aircraft loading during flight, can be performed with permanent increase of the maximum stress level from one cycle to another (see Fig.8c). A two-parameter model for load interaction effects, including the size of the stretch zone, d_{st}, was used to estimate the fatigue crack increment under an overload in the case discussed. A block of cyclic loads obtained from stress-state analysis of several flights for a wing area of the Yak-42 civil aircraft was examined, Fig.8c. The biaxial stress ratio was in the range of -0.2< λ <+0.5 for 55 cyclic loads in the schematic block for one flight.

Measurements performed earlier have shown a correlation between the stretch zone size and the equivalent stress intensity factor, K_e, in the range of –1.0< λ <+1.0 and 0.1<R <0.8 Shanyavskiy [9,10]. Based on these measurements the mean value, d_{st}, of the stretch zone was expressed as $d_{st} = C_o + C_1 K_e$, where factors, C_0 and C_1 were determined from the results of cruciform specimen tests. For D16T Al-alloy subjected to biaxial cyclic loads the stretch zone value was measured, Shanyavskiy [9], and d_{st}-value versus K_e was constructed. The sequence of events during one cycle of loading for simulated fatigue cracking was considered based on the following relations, which includes the static jump increment, $d_{\dim}$, and striation spacing, δ:

$$(\Delta_f) = d_{st} + d_{\dim} + \delta, \quad \text{for } (K_e)_{i+1} \ge (K_e)_i, \tag{15}$$

$$(\Delta_f) = \delta, \quad \text{for } (K_e)_{i+1} \le (K_e)_i, \tag{16}$$

Fatigue crack growth simulations using Eqs. (15) to (16) have shown that for the biaxial cyclic loads the crack increment because of stretch zone formation is dominant for

the cyclic loads sequence. In the case of biaxial tension-compression the crack growth period under the principal stress σ_1 = 70 MPa decreases by 4.5% (209 blocks of cyclic loads) in comparison with the case of σ_1 =0 for the crack interval 10-20mm. In the case of biaxial tension the crack growth period under the principal stress σ_1 = 70 MPa increases by 3.5% (160 blocks of cyclic loads) for the same crack growth interval.

In the case of crack growth rate in the region of more than 10^{-7} m/cycles, the crack increment after an overload must be simulated because of stretch zone formation and also because of fatigue striation spacing.

REFERENCES

1. Shanyavskiy, AA. (2003) *Tolerance fatigue cracking of aircraft structures. Synergetics in engineering applications*. Monography, Ufa, Russia.
2. Shanyavskiy, AA. (2005) In: *New Results in Fatigue and Fracture*, pp. 257–276, Kasprzak, W, Macha, E, Panasyuk, V, and Schaper, MK, (Eds), **1**. Mechanika No 300, Opole-Zakopane, Poland.
3. Shanyavskiy, AA. and Smikov, V.G. (1997) In: *Proc. of 5th Intern. Conf, Biaxial/Multiaxial Fatigue and Fract.*, pp.127-136, Macha, E., and Mroz, Z. (Eds), v. II, TUO, Poland.
4. Shanyavskiy, AA. and Koronov, M.Z. (1994) *Fatigue Fract. Engng Mater. Struct.* **9**, 1003-1013.
5. Shanyavskiy, AA., Orlov E.F. and Koronov M.Z. (1995) *Fatigue Fract. Engng Mater. Struct.* **11**, 1263-1276.
6. Shanyavskiy, AA. (1996) *Fatigue Fract. Engng Mater. Struct.* **19**, 1445-1458.
7. Miller, K.J. (1977) *Met. Sci.* **8/9**, 432-438.
8. Shanyavskiy, AA. and Orlov, E.F. (1997) In: *Proc. of 5th Intern. Conf, Biaxial/Multiaxial Fatigue and Fract.*, pp.137-148, Macha, E. and Mroz, Z. (Eds), v. II, TUO, Poland.
9. Shanyavskiy, AA. and Orlov, E.F. (1997) *Fatigue Fract. Engng Mater. Struct.* **20**, 151-166.
10. Shanyavskiy, AA. and Orlov, E.F. (1997) *Fatigue Fract. Engng Mater. Struct.* **20**, 1719-1730.
11. *Biaxial and Multiaxial Fatigue*, Brown, M.W. and Miller K.J., Eds. (1989) Europen Group on Fracture (ESIS) Publication 3; Bury St. Edmunds, Mechanical Engineering Publications.
12. Carpinteri, Andrea. (1994) In: *Chapter **18** of the book: Handbook of Fatigue Crack Propagation in Metallic Structures*, Edited by Andrea Carpinteri, Elsevier Science Publishers B.V., Amsterdam, Netherlands, 127-142.
13. Schijve, J. (1981) *Engng Fract. Mech*. **4**, 789-800.
14. Elber, W. (1970) *Engng Fract. Mech*. **1**, 37-45.

15. Shanyavskiy, AA., Orlov, E.F. and Grigoriev, V.M. (1997) *Fatigue Fract. Engng Mater. Struct.* **20**, 975-983.
16. Schijve, J. (1973) *Engng Fract. Mech*. **5**, 269-282.
17. Newman, J.C. (1981) In: *ASTM STP* **748**, 53-84.
18. Schijve, J. (1987) In: *Fatigue 87*, pp.1685-1722, EMSA, Vol. III.